Recognition-Aware HRRP Generation With Generative Adversarial Network

Yue Huang, *Member, IEEE*, Yi Wen, Liangchao Shi, and Xinghao Ding, *Member, IEEE*

***Abstract*— Existing works on radar high-resolution range profile (HRRP) recognition commonly focus on utilizing data and various deep learning models in achieving high classification accuracy. However, in practical applications, it is often difficult to obtain HRRP signals, especially for noncooperative targets. Such lack of data dramatically decreases the recognition performance, so this letter applies data augmentation to address small-sample problems. A recognition-aware HRRP generation framework based on a generative adversarial network is proposed for data augmentation, which generates discriminative samples by decomposing and reorganizing signal's characteristics. The proposed model increases the generated signals' discriminative power, thus meeting the application requirements. Experiments show that the generated HRRP signals can not only accurately expand the data set but also improve the recognition system's performance. Besides, the developed model outperforms traditional data augmentation methods and other generative methods. To the best of our knowledge, this is the first work on HRRP signal generation in radar automatic target recognition systems.**

***Index Terms*— Data generation, generative adversarial network (GAN), high-resolution range profile (HRRP), target recognition.**

I. Introduction

A High-resolution range profile (HRRP) is a 1-D scattering intensity distribution of a target radar echo that contains the target's attitude, size, and scattering information (see Fig. 1). Moreover, the HRRP signal is easy to store and has a low computational cost. As a result, target recognition via HRRP signal processing has gained considerable attention in recent years [1], [2]. For example, Wang *et al.* [3] proposed a scattering centers extraction method, which utilizes the scattering centers fuzzy matching for target recognition and achieves good results. Wang *et al.* [4] tackled the open-set problem by implementing the extreme value theory into the random forest classifier that can automatically detect the unknown classes.

When developing recognition models based on HRRP data, most of the works within the HRRP signals classification field exploited the deep neural networks' representative capabilities. The first HRRP recognition model based on deep learning was proposed in [5], which utilizes a multilayer nonlinear network based on stacked corrective autoencoders. Pan *et al.* [6] proposed a recognition framework that combines t-distributed stochastic neighbor embedding (t-SNE) and a discriminant deep belief network to improve the imbalanced data sets modeling. Further advances in classification performance were enabled by applying other deep model structures, for example, Liao *et al.* [7] used a concatenated deep neural network, Guo *et al.* [8] introduced a residual module, and Xu *et al.* [9] proposed an recurrent neural network (RNN)-based target-aware recurrent attentional network.

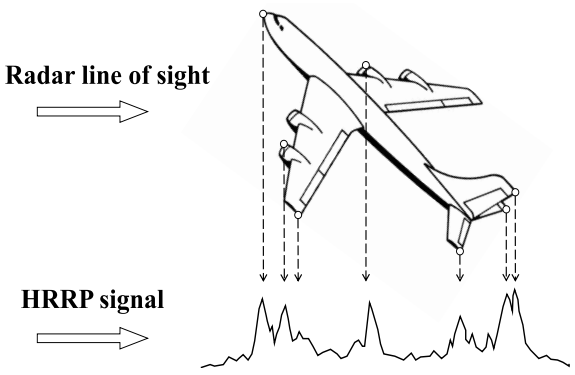

Fig. 1. Example of HRRP signal generated from an aircraft target, the circles on the target indicate the scattering centers.

Most of the existing contributions assume the existence of sufficient training data. However, in real-world scenarios, obtaining HRRP signals is often challenging, especially for noncooperative targets. In addition, capturing sufficient HRRP signals from all aspects is expensive. The insufficiencies in training data can significantly limit the deep learning performance on HRRP recognition tasks. Several works contributed to mitigating these data issues, such as HRRP estimation with stepped-frequency waveform [10], [11] and signal stimulation with electromagnetic software [12], [13], and they reconstructed HRRP signals by waveform synthesis and target modeling, respectively.

Data augmentation is widely considered an effective technique for improving deep learning models' accuracy. Many machine learning fields (e.g., computer vision) use traditional data augmentation methods, such as adding noise, shifting, and flipping. While these methods can also be applied in HRRP data augmentation, neither the semantic information hidden in HRRP signals nor the discriminative power has been considered to date.

Manuscript received August 13, 2020; revised December 9, 2020; accepted January 26, 2021. Date of publication February 12, 2021; date of current version December 17, 2021. This work was supported in part by the National Natural Science Foundation of China under Grant 81671766, Grant 61971369, Grant U19B2031, Grant U1605252, and Grant 61671309; in part by the Open Fund of Science and Technology on Automatic Target Recognition Laboratory under Grant 6142503190202; and in part by the Fundamental Research Funds for the Central Universities under Grant 20720180059, Grant 20720190116, and Grant 20720200003. *(Corresponding author: Xinghao Ding.)*

The authors are with the School of Informatics, Xiamen University, Xiamen 361005, China (e-mail: dxh@xmu.edu.cn).

Digital Object Identifier 10.1109/LGRS.2021.3056192

The generative adversarial network (GAN) [14] attracted significant attention within the computer vision field, especially in image translation tasks [15]–[17]. The GAN-based methods adaptively decouple the features and then perform the data style conversions between the domains.

This letter introduces the idea of image translation into the radar automatic target recognition (RATR) task that the feature transformation between the targets is used to augment the data of targets with insufficient samples. Moreover, since the traditional image translation technology does not explore the discriminative power hidden in the signals, this letter proposes a recognition-aware feature transformation network that decomposes signals into semantic information and pose information through content encoder and style encoder, respectively, and combines specific semantic encoding with other pose encoding to make generated samples more diverse. In order to enhance the discrimination of the generated samples, the semantic encoder is also served as a part of the discriminator.

The HRRP data generated by the proposed method largely differs from that estimated by waveform synthesis or simulated by electromagnetic calculation, which may have severe domain shifts from the real data, thus hampering the recognition tasks' performance. In contrast, the proposed method generates the signal from the real HRRP data, maintaining the original semantic characteristics and ensuring the generated data styles' diversity all of which are crucial for the RATR task.

This letter's contributions are summarized as follows.

1) The work tackles the described data issues by proposing a data augmentation framework that generates the HRRP signals from a limited real data set. To the best of the authors' knowledge, this is the first work on HRRP generation based on GAN.
2) This letter proposes a recognition-aware feature transformation network that generates discriminative and diverse HRRP samples, achieving accurate and effective data augmentation on the application level.
3) The experimental results demonstrate that the proposed model can effectively expand the data set, and the discriminant quality of the generated HRRP signals is better than other augmentation methods.

II. Methodology

A. Recognition-Aware HRRP Generation Network

This letter proposes an HRRP generation model based on image translation, i.e., a style transfer between two targets. Since the small-sample problem is mostly caused by the lack of the target's partial aspects, the proposed framework considers the pose information as the main feature to transform. First, the pose information from the target with complete aspects is obtained. The information is then converted into the target with missing aspects to enhance the missing aspects' characteristics and augment the data set effectively. The structure of the proposed model is shown in Fig. 2.

1) Intradomain Decomposition: Let $\boldsymbol{x}_1 \in \mathcal{X}_A$ and $\boldsymbol{x}_2 \in \mathcal{X}_B$ be samples from domains A and B. The two encoders mapping the samples into the feature spaces are denoted: $[c_i, s_i] = [E_c^i(\boldsymbol{x}_i), E_s^i(\boldsymbol{x}_i)], i = 1, 2$. where c_i and s_i stand for content and style encodings in domain i, respectively, thus containing the semantic and pose characteristics of the sample. E_c^i and E_s^i are corresponding encoders in domain i.

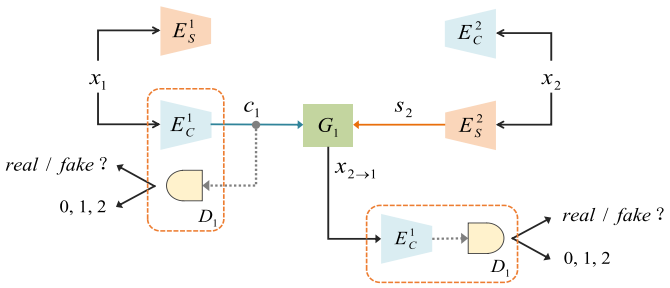

Fig. 2. Model structure for generating fake samples from domain B to A. x_1 and x_2 are input samples from each domain, E_c^i and E_s^i stand for content and style encoders, respectively, and G_1 and D_1 are generator and discriminator, respectively. The blue arrow represents the semantic encode, the orange arrow represents the pose encode, and the gray dotted arrow represents the code discriminant process.

2) Cross-Domain Generation: Cross-domain generator reorganizes the semantic and pose features across two domains. For example, when generating a fake sample in domain A, content code c_1 of $\boldsymbol{x}_1$ sample and style code s_2 of $\boldsymbol{x}_2$ sample are combined to generate a fake sample $\boldsymbol{x}_1' = G_1(c_1, s_2)$. Now, $\boldsymbol{x}_1'$ contains semantic and pose features of samples in A and B domains, respectively.

3) Discriminator: In addition to the content coding, the encoder E_c^i also serves as the feature extraction part of the discriminator, and thus, the discriminator can pay more attention to the quality of semantic features. In order to further improve the discrimination of generated signals, discriminator D_i not only needs to determine the authenticity of the input code but also needs to output the category the encoding belongs to.

B. Model Optimization and Loss Function

As before, let $\boldsymbol{x}_1$ and $\boldsymbol{x}_2$ be samples from two domains. Furthermore, let $p(\boldsymbol{x}_1)$ and $p(\boldsymbol{x}_2)$ denote their corresponding distributions. The network's loss function includes three parts: adversarial, reconstruction, and cycle loss. Suppose that the data are transformed from domain B to domain A.

1) Adversarial Loss: An adversarial training mechanism consists of a generator and a discriminator. Generator G_1's goal is to maximize the generated samples' realism, whereas discriminator D_1 aims at distinguishing the real samples from the false ones. The two are iteratively trained and are strengthened by each other

$$\mathcal{L}_{\text{adv}}^{2\to1} = \mathbb{E}_{\boldsymbol{x}_1\sim p(\boldsymbol{x}_1)}\left[\log D_1(\boldsymbol{x}_1)\right] + \mathbb{E}_{c_1=E_c^1(\boldsymbol{x}_1),s_2=E_s^2(\boldsymbol{x}_2)}\left[\log(1 - D_1(G_1(c_1, s_2)))\right].$$

In addition to identifying the real and fake samples, the discriminator performs classification. Thus, there is a classification loss for D_1

$$\mathcal{L}_{\text{cls}}^{2\to1} = \mathbb{E}_{\boldsymbol{x}_1\sim p(\boldsymbol{x}_1)}\left[\boldsymbol{y}_1 \log(D_1(\boldsymbol{x}_1))\right] + \mathbb{E}_{c_1=E_c^1(\boldsymbol{x}_1),s_2=E_s^2(\boldsymbol{x}_2)}\left[\boldsymbol{y}_1 \log(D_1(G_1(c_1, s_2)))\right]$$

where $\boldsymbol{y}_1$ stands for the one-hot encoding of $\boldsymbol{x}_1$'s real label.

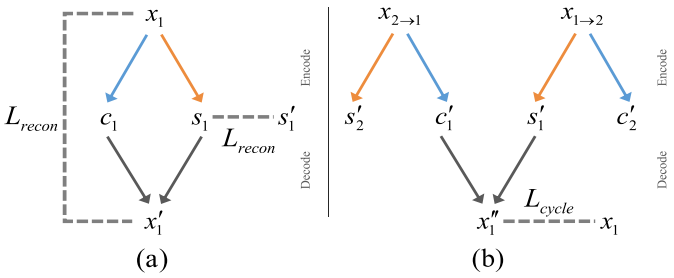

Fig. 3. Diagram of (a) reconstruction loss and (b) cycle loss. The gray bold dotted line represents the L_1 loss of data at two ends.

2) Reconstruction Loss: Reconstruction loss helps generator learns general HRRP probability distribution and maintains the distribution consistency between the samples before and after reconstruction. For the original sample $\boldsymbol{x}_1$, the method should be able to reconstruct the distribution from its content and style encodings. Moreover, the pose information of sample $\boldsymbol{x}_{1\to2}$ (generated from c_2 and s_1) should be consistent with s_1 after transformation. The measurement of two distribution is the L_1 distance

$$\mathcal{L}_{\text{recon}}^1 = \mathbb{E}_{\boldsymbol{x}_1\sim p(\boldsymbol{x}_1)}\left[\|\boldsymbol{x}_1 - G_1\left(E_c^1(\boldsymbol{x}_1), E_s^1(\boldsymbol{x}_1)\right)\|_1\right] + \mathbb{E}_{\boldsymbol{x}_1\sim p(\boldsymbol{x}_1)}\left[\|E_s^1(\boldsymbol{x}_1) - E_s^2(\boldsymbol{x}_{1\to2})\|_1\right].$$

3) Cycle Loss: Cycle loss retains the transformation stability between the two domains, increasing the independence and accuracy of feature decomposition and composition, and also regularizes the ill-posed translation problem. Once samples $\boldsymbol{x}_{2\to1}$ and $\boldsymbol{x}_{1\to2}$ in two domains have been generated, they are encoded to obtain the content code (i.e., $c_1' = E_c^1(\boldsymbol{x}_{2\to1})$) and the style code (i.e., $s_1' = E_s^1(\boldsymbol{x}_{1\to2})$), respectively. These two codes are combined to obtain the cycle sample $\boldsymbol{x}_1'' = G_1(c_1', s_1')$, which should be consistent with original sample $\boldsymbol{x}_1$. Thus

$$\mathcal{L}_{\text{cycle}}^1 = \mathbb{E}_{\boldsymbol{x}_{2\to1},\boldsymbol{x}_{1\to2}\sim p^*(.)}\left[\left\|\boldsymbol{x}_1 - G_1(E_c^1(\boldsymbol{x}_{2\to1}), E_s^2(\boldsymbol{x}_{1\to2}))\right\|_1\right]$$

where $p^*(.)$ denotes the generated fake distributions.

The diagram of the reconstruction loss and cycle loss is shown in Fig. 3. The transformation from domain A to domain B is analogous. Thus, the total loss is calculated as follows:

$$\begin{aligned}\min_{G_1,G_2,E_s^1,E_s^2} \mathcal{L}\left(G_1, G_2, E_s^1, E_s^2\right) &= \lambda_{\text{gan}}\left(\mathcal{L}_{\text{adv}}^{2\to1} + \mathcal{L}_{\text{adv}}^{1\to2}\right) \\ &\quad + \lambda_{\text{recon}}\left(\mathcal{L}_{\text{recon}}^1 + \mathcal{L}_{\text{recon}}^2\right) \\ &\quad + \lambda_{\text{cycle}}\left(\mathcal{L}_{\text{cycle}}^1 + \mathcal{L}_{\text{cycle}}^2\right) \\ \min_{E_c^1,E_c^2}\max_{D_1,D_2} \mathcal{L}\left(E_c^1, E_c^2, D_1, D_2\right) &= \lambda_{\text{gan}}\left(\mathcal{L}_{\text{adv}}^{2\to1} + \mathcal{L}_{\text{adv}}^{1\to2}\right) \\ &\quad + \lambda_{\text{cls}}\left(\mathcal{L}_{\text{cls}}^{2\to1} + \mathcal{L}_{\text{cls}}^{1\to2}\right)\end{aligned}$$

where λ_{gan}, λ_{recon}, λ_{cycle}, and λ_{cls} are the generator's weight parameters.

Note that the content encoder is trained under the discriminator's objective, whereas the style encoder is trained under the generator's objective. The experiments discussed in Section III validate that such an optimization strategy enhances the generation and the discrimination processes' effectiveness.

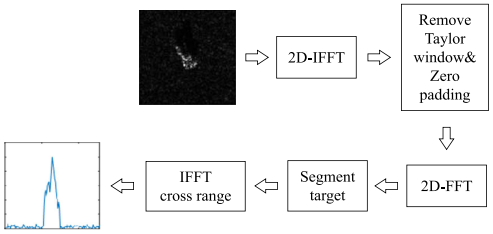

Fig. 4. Process of inverting HRRP signal from SAR image [18].

TABLE I
DATA SIZES OF DIFFERENT CASES IN TARGET 3

Obtained aspects	120	90	60	30
Training data	525	359	262	137
Training data after augmentation	1575	1077	786	411

III. EXPERIMENTAL RESULTS AND DISCUSSION

A. HRRP Data Introduction

Since the real HRRP data is difficult to collect, this work follows the approach used in [18], where the HRRP data are obtained from real synthetic aperture radar (SAR) images. Moving and stationary target automatic recognition (MSTAR) [19] is a public database that contains SAR images of ten ground target types. Within this work, three target types were randomly selected for validation: infantry fighting vehicles (Target 1), armored transport vehicles (Target 2), and tanks (Target 3).

The process of inverting the HRRP signal from SAR images is shown in Fig. 4. Due to the dimensions' nonuniformity and HRRP amplitude sensitivity, the experiments were preceded by data preprocessing. Zero padding was used at both sides of the sequence, dimension was unified to 201, and average linear normalization was used in intraframe normalization. More preprocessing details are available in [20].

B. Implementation Details

The data include 1165 HRRP signals for each target, covering 180 aspects from 1 to 180. For each target, 2/3 of the data were randomly selected as a training set, whereas the remaining data were used as a testing set. The training set served to generate HRRP signals, whereas the testing set validated the augmentation performance.

To simulate an insufficient data scenario, Targets 1 and 2 were assumed to have sufficient data, whereas Target 3 had missing data. Specifically, for Target 3, several aspects were randomly selected and reserved as a training set, whereas others were regarded as missing. Data removal is simulated in four cases, as shown in Table I.

The proposed model augments the insufficient training data for Target 3 using the knowledge transferred from the two auxiliary targets (Targets 1 and 2) with sufficient data (i.e., data covering all aspects). Target 3 serves as domain A, whereas Targets 1 and 2 represent domain B. Through the feature transformation between two domains, the fake samples of

TABLE II
BACKBONE OF THE CLASSIFIER

Layers	Conv1	Conv2	Conv3	Conv4	Conv5	FC1	FC2
#Filters	128	256	256	512	1024	1024	1024
Filter size	(1,32)	(1,32)	(1,8)	(1,8)	(1,4)	(1,4)	(1,1)

TABLE III
CLASSIFICATION OF THE PROPOSED METHOD'S TEST RESULTS. GAN AUGMENTED MEANS ADD THE GENERATED DATA OF TARGET 3 TO THE TRAINING SET

Accuracy(%)	Obtained aspects of Target 3			
(F-value of Target 3)	120	90	60	30
Basic	94.45(0.93)	89.34(0.84)	86.77(0.75)	78.86(0.54)
GAN augmented	96.82(0.95)	91.58(0.86)	89.80(0.81)	80.93(0.60)

Target 3 generated from the Targets 1 and 2 are combined as the augmented data of Target 3. Since the discriminator determines the content code category, it is necessary to introduce the two domains' category labels during the training procedure.

The proposed GAN model contains the content encoder composed of two down-sampling layers and four res-layers to obtain a 51-D content encoding. Furthermore, the style encoder uses six conv-layers to get a 32-D style encoding. The generator consists of four res-layers and two up-sampling layers. The discriminator consists of four conv-layers, followed by one conv-layer and one fc-layer corresponding to identification and results' classification, respectively. The classifier structure is shown in Table II.

All the experiments were implemented with TensorFlow. Other configuration details were as follows: the CPU was an Intel i7-7800X, the system memory was 64 GB, the graphics card was an NVIDIA GTX 1080Ti, and the model had a batch size of six and a learning rate of 1e−4.

C. Experimental Validation

The three-category classification is used to validate the generated HRRP signals' quality. As shown in Table III, labels "Basic" and "GAN augmented" denote performances before and after the Target 3 data augmentation, accuracy, and the F-value (Target 3) are used as validation metrics.

One can observe that the classification performance decreases dramatically with the decrease in the Target 3 training set size. On the other hand, data augmentation promoted improvements in the performance across all cases regarding both accuracy and F-value. These results demonstrate the positive effects of the Target 3 data augmentation on performance.

In the case where only 60 angles of Target 3 were obtained, the t-SNE analysis was used to visualize the test data features' distribution extracted by the classifier. As shown in Fig. 5, utilizing the proposed augmentation method significantly improves the classifier's ability to recognize the Target 3 data.

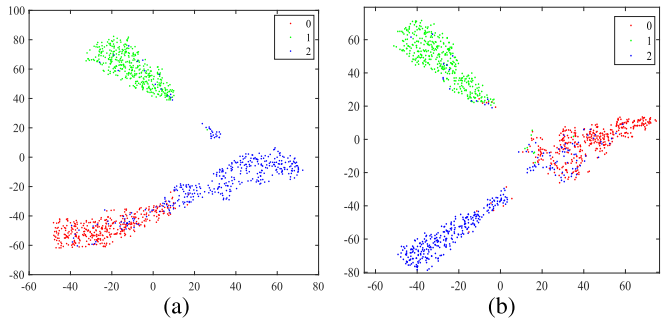

Fig. 5. t-SNE distribution of test set's feature before and after augmentation in 60 angles obtained case, and the 0, 1, 2 in the legend represents Targets 1–3. (a) Basic distribution. (b) After augmentation.

TABLE IV
COMPARISON OF DIFFERENT HRRP AUGMENTATION METHODS. THE BEST PERFORMANCE IS EMPHASIZED IN BOLD

Accuracy(%)		Obtained aspects of Target 3			
		120	90	60	30
Basic		94.45	89.34	86.77	78.86
Traditional methods	Adding noise	95.96	89.35	85.39	80.70
	Shifting	96.47	90.54	87.54	81.10
	Flipping	94.32	90.63	86.59	79.18
Other GAN methods	CGAN	95.18	90.55	87.55	78.52
	ACGAN	93.29	90.63	86.34	78.15
	CycleGAN	96.22	91.56	86.42	80.52
	MUNIT	93.72	90.18	88.06	80.28
Ours		**97.34**	**92.18**	**90.98**	**82.47**

D. More Comparisons

This section compares the proposed model's performance to traditional data augmentation methods (adding noise, shifting, and flipping) and other GAN methods. Gaussian noise with 0.1 variance and zero mean was used. The utilized shifting operation randomly shifted the HRRP signal 0?0 points to left or right. The flipping operation flipped the signal in both horizontal and vertical directions. The considered GAN models include the traditional GAN models (conditional GAN (CGAN) [21] and auxiliary classifier GAN (ACGAN), extends the discriminator to a classifier to control the pattern of the generated image [22]) and the GAN models based on image translation (CycleGAN [15] and multimodal unsupervised image-to-image translation (MUNIT) [16]). The generated Target 3 samples are kept doubling the training samples' amount.

As shown in Table IV, the proposed GAN-based augmentation method outperforms the traditional augmentation methods across all cases. In cases where numerous data are missing, traditional GAN models (i.e., CGAN and ACGAN) are less successful than the models based on image translation (i.e., CycleGAN and MUNIT). The proposed model focuses on the discrimination of the generated data and achieves the best feature conversion results, outperforming other GAN models.

Finally, the four loss functions used in the model (i.e., adversarial loss—GAN, reconstruction loss—recon, cycle loss—

TABLE V

PERFORMANCE COMPARISONS OF VARIOUS COMBINATIONS OF LOSS FUNCTIONS. THE BEST PERFORMANCE IS EMPHASIZED IN BOLD

Accuracy(%)	Obtained aspects of Target 3	
	120	60
Basic	94.45	86.77
recon+cycle+cls	95.46	86.98
GAN+cycle+cls	96.04	88.14
GAN+recon+cls	95.88	88.65
GAN+recon+cycle	94.76	67.96
Ours	**96.82**	**89.80**

cycle, and classification loss—cls) are studied. As shown in Table V, the experiment explores the impact of missing one of the four loss functions on the augmentation performance in cases where only 120 and 60 angles of Target 3 were obtained. The results show a drop in performance if any function is left out, highlighting the proposed model's advantages.

IV. CONCLUSION

In practical applications, insufficiencies in HRRP data significantly hamper the RATR task performance. Therefore, advancing the theoretical knowledge on deep learning for HRRP recognition may be insufficient, and the problem needed to be tackled from the data perspective. This work introduced a recognition-aware feature transformation network that generates discriminative samples by decomposing and reorganizing signal's characteristics. Experimental results prove that, in missing samples' cases, the proposed method can effectively improve the recognition performance by generating discriminant data and outperforms other augmentation methods. This letter is the first to combine the GAN model with the RATR task, effectively mitigating limitations caused by the lack of data. Finally, this work offers a new approach to small HRRP sample identification.

REFERENCES

[1] Z. Yun, T. Xuelian, L. Benyong, and W. Xueang, "Radar target recognition based on KLLE and a KNRD classifier," *WSEAS Trans. Signal Process.*, vol. 2, no. 6, pp. 47–57, 2010.

[2] L. Du, H. Liu, and Z. Bao, "Radar HRRP statistical recognition: Parametric model and model selection," *IEEE Trans. Signal Process.*, vol. 56, no. 5, pp. 1931–1944, May 2008.

[3] Y. Wang, L. Zhang, S. Wang, T. Zhao, Y. Wang, and Y. Li, "Radar HRRP target recognition using scattering centers fuzzy matching," in *Proc. CIE Int. Conf. Radar (RADAR)*, Oct. 2016, pp. 1–5.

[4] Y. Wang, W. Chen, J. Song, Y. Li, and X. Yang, "Open set radar HRRP recognition based on random forest and extreme value theory," in *Proc. Int. Conf. Radar (RADAR)*, Aug. 2018, pp. 1–4.

[5] B. Feng, B. Chen, and H. Liu, "Radar HRRP target recognition with deep networks," *Pattern Recognit.*, vol. 61, pp. 379–393, Jan. 2017.

[6] M. Pan, J. Jiang, Q. Kong, J. Shi, Q. Sheng, and T. Zhou, "Radar HRRP target recognition based on t-SNE segmentation and discriminant deep belief network," *IEEE Geosci. Remote Sens. Lett.*, vol. 14, no. 9, pp. 1609–1613, Sep. 2017.

[7] K. Liao, J. Si, F. Zhu, and X. He, "Radar HRRP target recognition based on concatenated deep neural networks," *IEEE Access*, vol. 6, pp. 29211–29218, 2018.

[8] C. Guo, Y. He, H. Wang, T. Jian, and S. Sun, "Radar HRRP target recognition based on deep one-dimensional residual-inception network," *IEEE Access*, vol. 7, pp. 9191–9204, 2019.

[9] B. Xu, B. Chen, J. Wan, H. Liu, and L. Jin, "Target-aware recurrent attentional network for radar HRRP target recognition," *Signal Process.*, vol. 155, pp. 268–280, Feb. 2019.

[10] A. Aubry, V. Carotenuto, A. De Maio, and L. Pallotta, "High range resolution profile estimation via a cognitive stepped frequency technique," *IEEE Trans. Aerosp. Electron. Syst.*, vol. 55, no. 1, pp. 444–458, Feb. 2019.

[11] P. Addabbo, A. Aubry, A. De Maio, L. Pallotta, and S. L. Ullo, "HRR profile estimation using SLIM," *IET Radar, Sonar Navigat.*, vol. 13, no. 4, pp. 512–521, Apr. 2019.

[12] T. Zhao, C.-Z. Dong, H.-M. Ren, and H.-C. Yin, "The radar echo simulation of moving targets based on HRRP," in *Proc. IEEE Int. Conf. Green Comput. Commun. IEEE Internet Things IEEE Cyber, Phys. Social Comput.*, Aug. 2013, pp. 1580–1583.

[13] Z. Wei, M. O. Cui-Qiong, C. Qiu-Ju, and C. Hui, "Modeling and simulation of radar HRRP to ship targets," *Electron. Opt. Control*, vol. 23, no. 2, pp. 47–50, 2016.

[14] I. J. Goodfellow *et al.*, "Generative adversarial networks," in *Proc. Adv. Neural Inf. Process. Syst.*, vol. 3, 2014, pp. 2672–2680.

[15] J.-Y. Zhu, T. Park, P. Isola, and A. A. Efros, "Unpaired image-to-image translation using cycle-consistent adversarial networks," in *Proc. IEEE Int. Conf. Comput. Vis. (ICCV)*, Oct. 2017, pp. 2242–2251.

[16] X. Huang, M.-Y. Liu, S. Belongie, and J. Kautz, "Multimodal unsupervised image-to-image translation," in *Proc. Eur. Conf. Comput. Vis. (ECCV)* (Lecture Notes in Computer Science), vol. 11207. 2018, pp. 179–196.

[17] R. Chen, W. Huang, B. Huang, F. Sun, and B. Fang, "Reusing discriminators for encoding: Towards unsupervised image-to-image translation," in *Proc. IEEE/CVF Conf. Comput. Vis. Pattern Recognit. (CVPR)*, Jun. 2020, pp. 8165–8174.

[18] D. C. Gross, M. W. Oppenheimer, B. Kahler, B. L. Keaffaber, and A. L. Williams, "Preliminary comparison of high-range resolution signatures of moving and stationary ground vehicles," *Proc. SPIE*, vol. 4727, pp. 205–213, Aug. 2002.

[19] Defense Advanced Research Projects Agency(DAPRA). *Moving and Stationary Target Automatic Recognition(MSTAR) Program*. Accessed: Nov. 8, 2018. [Online]. Available: https://www.sdms.afrl.af.mil/index.php?collection=mstar

[20] Y. Wen, L. Shi, X. Yu, Y. Huang, and X. Ding, "HRRP target recognition with deep transfer learning," *IEEE Access*, vol. 8, pp. 57859–57867, 2020.

[21] M. Mirza and S. Osindero, "Conditional generative adversarial nets," 2014, *arXiv:1411.1784*. [Online]. Available: https://arxiv.org/abs/1411.1784

[22] A. Odena, C. Olah, and J. Shlens, "Conditional image synthesis with auxiliary classifier GANs," in *Proc. Int. Conf. Mach. Learn. (ICML)*, vol. 70, 2017, pp. 2642–2651.